

Forschungszentrum Karlsruhe

in der Helmholtz-Gemeinschaft

Wissenschaftliche Berichte

FZKA 6745

Cryosorbent Characterization of Activated Charcoal in the COOLSORP Facility

Final Report on Subtask 8 of Task VP1: Cryopump Development and
Testing (ITER Task no. 448)

V. Hauer, Chr. Day

Institut für Technische Physik
Programm Kernfusion
Assoziation EURATOM-FZK

Forschungszentrum Karlsruhe GmbH, Karlsruhe
2002

Impressum der Print-Ausgabe:

**Als Manuskript gedruckt
Für diesen Bericht behalten wir uns alle Rechte vor**

**Forschungszentrum Karlsruhe GmbH
Postfach 3640, 76021 Karlsruhe**

**Mitglied der Hermann von Helmholtz-Gemeinschaft
Deutscher Forschungszentren (HGF)**

ISSN 0947-8620

Abstract

At Forschungszentrum Karlsruhe, a special cryovacuum pump system is being developed for use in the ITER nuclear fusion reactor. At the operation temperature of about 5 K, practically all gases can be condensed easily, except of helium and hydrogen isotopes. To bind these species as well, the panels are coated with sorbent materials. Best pumping characteristics are achieved with activated charcoal. For the basic design of such cryosorption pumps, isotherm data are strongly needed, which are extremely scarce, especially at temperatures between 4.2 K (LHe) and 77.3 K (LN₂). Therefore, the novel continuous sorption device COOLSORP was developed to measure sorption characteristics up to atmospheric pressure under variable temperature cryogenic conditions. The facility is based on a commercially available pore-analyser (continuous sorption method), upgraded by a heatable closed He cycle two-stage Gifford McMahon refrigerator.

This report gives an overview about the experimental programme performed over the last two years. For qualification of the new facility and for comparison reason, standard measurements with nitrogen at 77 K were performed. However, the emphasis of the experimental was placed on low temperature sorption isotherms (experimental and correlated data) of gases with special relevance for cryosorption vacuum pumping, like helium and hydrogen, in both the sub- and the supercritical temperature range, whenever possible. The parametric measurements were focussed on a special, commercially available, granular coconut-shell based charcoal (CHEMVIRON SC 2), which was shown to have excellent vacuum pumping performance and, thus, has become the candidate for nuclear fusion application (ITER reference material).

Prior to the measurements, preliminary tests were driven to set the facility into operation properly, to confirm the applicability of the experimental method used and to calibrate the measuring instruments. Pore size information was then derived from the measured isotherms. The standard models (Langmuir, Brunauer, Emmett and Teller, Dubinin-Radushkevich) were applied for analysis of the measurement data (micro- and mesopore volume, surface area). The Density Functional Theory approach was employed to derive pore size distributions from the 77 K nitrogen isotherms. It is revealed how the accessible pore size and volume depend on the adsorptive under investigation. It is also shown that the use of standard models (recommended for nitrogen) may produce ambiguous results when applied to other gases such as helium or hydrogen. The experimental results presented in this report are especially needed to have a data base which could be used for benchmarking any new sorbent material for cryosorption pumping use.

Charakterisierung der Tieftemperatursorption auf Aktivkohle mit der Anlage COOLSORP

Zusammenfassung

Am Forschungszentrum Karlsruhe wurde und wird weiterhin ein Kryopumpensystem für die Verwendung im ITER-Fusionsreaktor entwickelt. Mit Kryopumpen kann bei einer Arbeitstemperatur von 5 K nahezu jedes Gas kondensiert werden, mit Ausnahme von Helium und den Wasserstoffisotopen. Um diese ebenfalls zu binden, müssen die Kryopanele der Pumpen mit Sorptionsmaterial beschichtet werden. Die besten Pumpeigenschaften zeigt dabei Aktivkohle. Für das Design einer solchen Kryopumpe ist es wichtig, die Sorptionscharakteristik der zu verwendenden Aktivkohle im interessanten Temperaturbereich zwischen 4,2 K (LHe) und 77,3 K (LN₂) zu kennen. Die dazu benötigte Anlage zur kontinuierlichen Messung der Sorption bei unterschiedlichen Temperaturen bis zu Umgebungsdruck wurde mit COOLSORP verwirklicht. Diese Anlage basiert auf einem kommerziell erhältlichen Porenanalysegerät (kontinuierliches volumetrisches Verfahren), das durch einen heizbaren, zweistufigen Gifford-McMahon-Refrigerator erweitert wurde.

Der Bericht gibt einen Überblick über das Versuchsprogramm der letzten zwei Jahre. Die ersten Messungen, zum Testen der Anlage und als Vergleich zu anderen Autoren, wurden mit Stickstoff bei 77 K durchgeführt. Jedoch liegt der Schwerpunkt auf der Bestimmung von Adsorptionsisothermen (experimentell oder korreliert) von Gasen bei tiefen Temperaturen. Interessant sind Isothermen von Gasen, die nur durch Kryosorption gebunden werden können, wie Helium und die Wasserstoffisotope, wenn möglich im sub- und superkritischen Bereich. Die durchgeführten Untersuchungen wurden auf eine kommerziell erhältliche, granulare, aus Kokosnuss gewonnene Aktivkohle (CHEMVIKON SC2) beschränkt. Sie zeichnet sich durch ein exzellentes Saugvermögen aus und ist für die Verwendung im ITER-Fusionsreaktor vorgesehen.

Vor den eigentlichen Messungen wurden verschiedene Voruntersuchungen durchgeführt. Neben der Funktionsprüfung der Anlage und der Messmethode wurden alle Messinstrumente kalibriert. In den folgenden Messungen wurden für die verschiedenen Gase und Temperaturen Isothermen erstellt, die Basis für die Porengrößenanalyse waren. Dabei kamen Standardverfahren wie Langmuir, Brunauer-Emmett-Teller und Dubinin-Radushkevich für die Berechnung von Mikroporen- und Mesoporenvolumina und inneren sowie äußeren Oberflächen zur Anwendung. Weiterhin wurde die Dichtefunktionaltheorie (DFT) zur Bestimmung der Porenverteilung genutzt. Hier ist die Abhängigkeit von untersuchtem Adsorptiv und nutzbarer Porengröße als auch Porenvolumen interessant. Es wird gezeigt, dass die Anwendung von Standardmodellen (wie für Stickstoff empfohlen) für andere Gase (z. B. Helium, Wasserstoff) zu unbefriedigenden Ergebnissen führt. Die hier gezeigten Ergebnisse bilden die Basis für die Beurteilung anderer Sorptionsmittel für den Einsatz in Kryopumpen.

Contents

1	Introduction	5
2	Basic Principles	6
2.1	Porous Substances	6
2.1.1	Activated Carbon	6
2.2	Adsorption	7
2.3	Evaluation Approaches	9
2.3.1	Langmuir Isotherm	9
2.3.2	BET Isotherm	10
2.3.3	Dubinin-Radushkevich Isotherm	11
2.3.4	t-plot	11
2.3.5	Density Functional Theory (DFT)	12
2.4	Conclusion	13
3	Experimental Setup	14
3.1	Substances Studied	14
3.1.1	Activated Carbon	14
3.2	Gases Used	14
3.3	Measurements	15
3.4	Experimental Setup	15
3.4.1	OMNISORP Unit	15
3.4.2	Refrigerator Unit	17
3.5	Experimental	18
3.5.1	Evaluation of the Measured Results	20
3.6	Operational Studies	21
3.6.1	Calibration	21
3.6.2	Studies with the Cryohead	22
3.7	Blank Measurements	25
3.8	Dependence on the Flow Rate	26
3.9	Encountered Problems	27
4	Results	29
4.1	Studies with Nitrogen	29
4.1.1	Adsorption Isotherms	29
4.1.2	Langmuir Plot	30
4.1.3	BET Plot	30
4.1.4	Dubinin-Radushkevich Plot	31
4.1.5	t-plot	33
4.1.6	Density Functional Theory	33
4.1.7	Summary of the Studies with Nitrogen	35
4.2	Studies with Helium	36
4.2.1	Adsorption Isotherms	36

4.2.2	Langmuir Plot	36
4.2.3	BET Plot	37
4.2.4	Dubinin-Radushkevich Plot	37
4.2.5	Summary of the Studies with Helium	38
4.3	Studies with Hydrogen	39
4.3.1	Langmuir Plot	40
4.3.2	Dubinin-Radushkevich Plot	41
4.3.3	Summary of the Studies with Hydrogen	42
5	Summary and Outlook	43

1 Introduction

The physisorption of gases in highly porous substances at cryogenic temperatures is a common technique of vacuum generation for those gases which cannot be condensed even at the very low temperatures of about 4 K (liquid helium conditions). The cryosorption pumps used for this purpose are accumulation pumps characterized by their high pumping speed, very low end pressure, and excellent storage capacity. These characteristics are achieved by optimum coating of the pumping surfaces, among other things. Mainly zeolite and activated carbon are used for this purpose. Activated carbon has the advantage over zeolite of being hydrophobic, which results in a comparatively better adsorption behavior to other gases in the presence of residual moisture. Carbon also needs considerably lower activation temperatures. Being a natural product, activated carbon suffers from the bad reproducibility of various properties, such as pore distribution and pore size. This makes the characterization of activated carbon more difficult, and requires more detailed studies.

If large quantities of hydrogen (all six hydrogen isotopes) and helium are to be pumped by cryopumps, as planned in future fusion experiments such as ITER (International Thermonuclear Experimental Reactor), competing sorption between the gases must be borne in mind. Assuming a sticking probability of 0.1 to 0.2 for helium, and between 0.6 and 0.95 for the different hydrogen isotopes, there is a need for an activated carbon species with the highest possible sticking probability for helium or high sorption capacity in general. For this purpose, characteristics of the activated carbon foreseen for ITER, at the planned operating temperatures and for the most important gases encountered must be found. Within the Deliverable 8 of EU Task VP1, Cryopump Development and Testing, measurements have therefore been conducted with helium and hydrogen at various temperatures.

The basis of these activities is the COOLSORP sorption measuring facility. It constitutes an advanced version of the OMNISORP 100 test facility, to which a low-temperature unit has been added. One special objective in the development of the COOLSORP facility was to get a universal tool for qualitative and quantitative analysis of any sorbent material and to compare the performance data with these of well-known materials. This could become especially important, if the chosen material would no longer be available by the industrial production company.

This report indicates the state of work with respect to studies conducted, problems encountered, and also represents a summary of the findings made so far.

2 Basic Principles

2.1 Porous Substances

A substance is referred to as porous if a sizable part of its total volume is taken up by pores. These pores may be open, i.e. connected to the outer surface of the substance, or closed. Only open pores play a role in adsorption studies, because others are not reached by the fluid under study. The inner pore surface area can attain levels of a few 1000 m²/g in porous substances. The volume enclosed by the pores is in a range between a few thousandths and a few ml/g. Next to the pore volume, also the size of pores is of interest in adsorption studies. As a consequence of different adsorption mechanisms, and for better distinction among the pore widths encountered, these have been subdivided into four categories by the International Union of Pure and Applied Chemistry (IUPAC) [1].

Table 1: Classification of Pores according to IUPAC [1]

Submicropores			$w < 0.8 \text{ nm}$
Micropores	$0.8 \text{ nm} < w < 2.0 \text{ nm}$		
Mesopores	$2.0 \text{ nm} < w < 50.0 \text{ nm}$		
Macropores	$50.0 \text{ nm} < w$		

The substances used to adsorb gases and liquids exhibit very different pore distributions. All-synthetic materials, such as zeolite, have narrow pore distributions with pore widths of a few Ångstrom. Activated carbon and other materials produced from natural substances exhibit a wider pore distribution which may vary greatly as a function of the manufacturing technique employed [1].

2.1.1 Activated Carbon

Activated carbon is a term encompassing graphite-like, partly microcrystalline carbon species. A characteristic feature of activated carbon is the large inner pore surface area resulting from the high porosity. Consequently, activated carbon is used in the adsorption of various organic and inorganic substances from gases, vapors, and liquids. In addition to cleaning air, gas, and sewage, it is used, inter alia, for decolorizing and cleaning a variety of liquids in the food industry, in catalytic reactions in the chemical industry, for enriching metals and metallic compounds in the mining and smelting industries, in medical technology, and this is what interests us most, in vacuum technology [2].

Activated carbon is made out of vegetable matter rich in carbon (e.g. charcoal, lignite or hard coal, cane sugar, coconut shells, fruit pips), animal waste (e.g. bones, blood), and final products of the oil processing industry (e.g. bitumen). Before being used as a sorbent, the basic material must be activated while or after being heated in the absence of air. In addition, the basic material can be added an extraneous substance easy to dissolve out prior to heating (such as zinc chloride) to avoid the carbon from sintering

together. Subsequent activation can be achieved by passing water vapor ($C + H_2O \rightarrow CO + H_2$), air ($C + \frac{1}{2}O_2 \rightarrow CO$) or carbon dioxide-bearing gases ($C + CO_2 \rightarrow 2CO$) at 700–900 °C [3].

Activated carbon consists primarily of graphite crystallites which, in turn, comprise 3–4 parallel carbon layers. The distance between the layers is 3.44 to 3.65 Å, which is slightly larger than in graphite (3.354 Å). The layers, with an approximate diameter of 20–25 Å, are made up of the six-membered ring carbon surfaces typical of graphite. However, unlike their arrangement in graphite, they are positioned irregularly. In addition to graphite crystallites, activated carbon can contain one to two thirds amorphous carbon and a variety of heteroatoms, such as oxygen and hydrogen.

The porous structure of activated carbon results from the irregular arrangement of the different graphite crystallites and amorphous fractions. The voids between the particles (pores) can have inner diameters between approx. 10^{-2} and 10^5 Å. The distribution and arrangement of pore widths has a decisive impact on the adsorption and diffusion of the materials considered [2].

2.2 Adsorption

When a solid is exposed to a gas in a vacuum, this gas adsorbs as a function of the chemical properties of the gas (adsorptive) and the solid (adsorbent), and also of the physical properties of the measuring system considered (e.g. pressure, temperature, volume). The adsorbed gas (adsorbate) results in a pressure reduction as well as an increase in mass of the solid in the enclosed volume. These effects are exploited in volumetric and gravimetric measuring techniques. In accordance with the measuring technique opted for, the quantity adsorbed is determined from the amount of gas admitted or from the change in weight of the adsorbent.

The plot of the volume adsorbed, the amount of substance, or mass versus the measured pressure or the relative pressure (quotient of the measured pressure and the saturation vapor pressure at measurement temperature) is called the adsorption isotherm. From the phenomenological point of view, according to the IUPAC, it can be classified in one out of six classes (Fig. 1).

The type-I adsorption isotherm is characterized by a concave shape, a steep rise at low relative pressures, and a pronounced plateau. The steep rise is interpreted as an indication of pronounced microporosity (pore width below 2 nm), while the plateau is interpreted as a sign of a small external surface of the adsorbent. Adsorption is limited by the micropore volume.

The type-II isotherm exhibits a concave shape only at low relative pressures, which is followed by a linear range which, in turn, is followed by a slightly convex shape at relative pressures close to unity. This shape results when the adsorbate layer grows quickly as the relative pressure rises. When saturation vapor pressure is reached, the adsorbate changes into the liquid or solid phase. The beginning of the linear range can be interpreted as the completion of an adsorbed monolayer and as a transition to multi-layer adsorption. Type-II adsorption isotherms are attributed to non-porous and macroporous substances (pore width in excess of 50 nm).

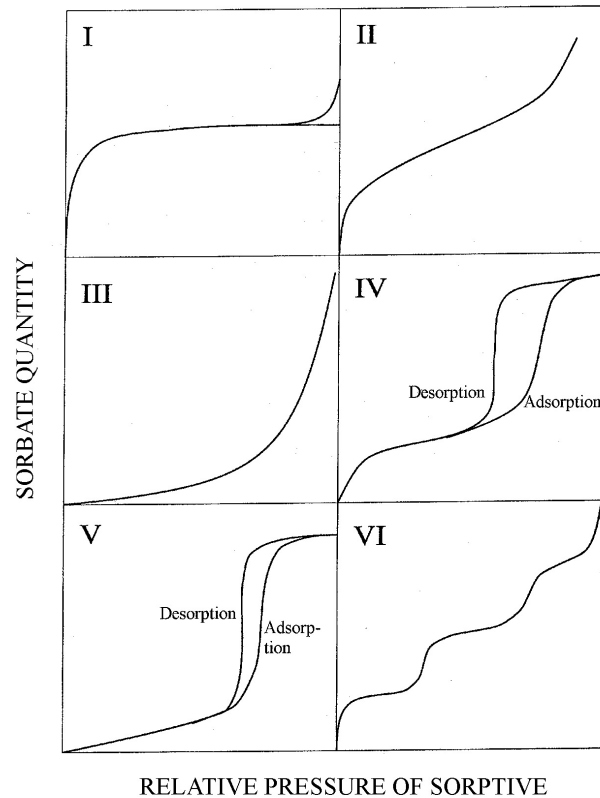


Figure 1: Classification of adsorption isotherms according to IUPAC [4].

Type-IV isotherms are similar to those of type II. The difference results from the existence of hysteresis, which indicates the presence of mesopores (pore width between 2 and 50 nm) filling and emptying by capillary condensation and evaporation, respectively, and arises from the faster desorption, compared to adsorption, at high relative pressures. The shape of the hysteresis loop partly differs greatly from adsorbent to adsorbent. IUPAC has classified four basic forms of hysteresis for studies of such isotherms (Fig. 2).

Type-III and type-V isotherms show pronounced convex slope, thus revealing a weak interaction between the adsorbate and the adsorbent. Type-V isotherms differ from type-III adsorption isotherms by reaching saturation pressure and in the existence of hysteresis. The hysteresis loop is indicative of a porous adsorbent.

The type-VI adsorption isotherm is called step isotherm. The steps show the adsorption of individual layers, whose formation is a function of the adsorbate-adsorbent system and of temperature.

Most of the adsorbents used in practice show adsorption isotherms which cannot be clearly assigned to any one type, especially with highly porous substances with vastly different pore widths. For studies of our activated carbon, therefore, a pure type-I isotherm and a combination of type-I and type-II or type-IV isotherms, respectively, were assumed [5].

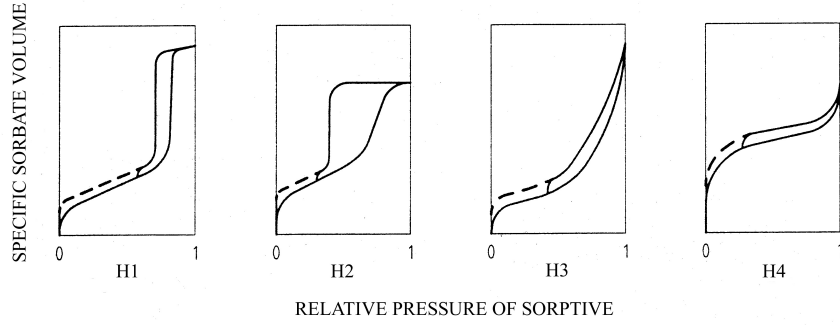


Figure 2: IUPAC hysteresis shapes for type-IV adsorption isotherms [4].

2.3 Evaluation Approaches

A large number of approaches based on kinetics, thermodynamics and/or empiricism are available for the interpretation and further evaluation of adsorption isotherms. A very simple formulation of the relationship between the adsorbed quantity and pressure is the adsorption isotherm according to Henry [2]:

$$V_{ads} = k \cdot p. \quad (1)$$

V_{ads} refers to the volume adsorbed, k is a constant dependent on the adsorbent, the gas used, and the temperature, and p is the measured equilibrium pressure. Application of the Henry isotherm presupposes ideal behavior of the gas, which can be assumed to exist only at correspondingly low pressures and appropriately high temperatures (supercritical range).

2.3.1 Langmuir Isotherm

The isotherm equation indicated by Langmuir can be used for homogeneous adsorbent surfaces and negligible interaction among the adsorptive molecules:

$$V_{ads} = V_{mono} \cdot \frac{kp}{1 + kp}. \quad (2)$$

For very low pressures, kp is much smaller than 1, Eq. 2 converges into

$$V_{ads} = V_{mono} \cdot kp. \quad (3)$$

For high equilibrium pressures, the 1 in Eq. 2 can be neglected. In this way, the volume adsorbed corresponds to the volume of the monolayer:

$$V_{ads} = V_{mono}. \quad (4)$$

For practical handling, Eq. 2 is used in this form:

$$\frac{p}{V_{ads}} = \frac{1}{kV_{mono}} + \frac{p}{V_{mono}}. \quad (5)$$

Plotting p/V_{ads} against p produces a straight line with the slope of $1/V_{mono}$ and an additive constant of $1/kV_{mono}$ in the range of validity of the Langmuir equation ($V_{ads}/V_{mono} \leq 1$).

The specific surface, S_m , can be calculated by means of the two constants. It is the product of the adsorbate monolayer volume, V_{mono} , the mean value of the area covered per particle, A_m , and Avogadro's constant, N_A , relative to the molar volume, V_{mol} , at standard conditions (22.4 l/mol at 273.15 K and 1013.25 mbar):

$$S_m = \frac{V_{mono}A_mN_A}{V_{mol}}. \quad (6)$$

The value of A_m can be calculated from Eq. 7 by using the molar mass, M and the liquid density of the adsorbate, ρ_a :

$$A_m = f \left(\frac{M}{\rho_a N_A} \right)^{\frac{2}{3}}. \quad (7)$$

The geometry factor, f , depends on the adsorbate-adsorbent system. It is 1.091 for an assumed hexagonal packing. When this value is used for calculating the area, per particle, of nitrogen at 77 K, the result is the value of 0.162 nm² standardized by IUPAC. For other adsorbates, either a value for f must be determined or A_m must be taken from the literature [2, 6].

2.3.2 BET Isotherm

Also Brunauer, Emmett, and Teller presented a model describing adsorption processes on solid surfaces. It is based on the assumption of a monomolecular layer being formed which, as a consequence of the interactions among the adsorptive molecules, is covered with other layers during adsorption. In this way, it constitutes an extension of the Langmuir model based on a maximum of one adsorbate layer only. The basis of practical application of the BET method is the BET equation as written in this re-arranged way:

$$\frac{p/p_0}{V_{ads}(1-p/p_0)} = \frac{1}{V_{mono}C} + \frac{C-1}{V_{mono}C}p/p_0. \quad (8)$$

The equation contains the relative pressure, p/p_0 , the adsorbed volume, V_{ads} , the monolayer volume, V_{mono} , and the BET constant, C .

If $\frac{p/p_0}{V_{ads}(1-p/p_0)}$ is plotted versus p/p_0 and if a linear range is produced in the range of relative pressures between 0.05 and 0.3, linear regression may be used to calculate the rise, $\frac{C-1}{V_{mono}C}$, and the ordinate, $\frac{1}{V_{mono}C}$. The specific surface again is determined in accordance with Eq. 6.

The BET method can only be applied if linearity appears at a degree of coverage, V_{ads}/V_{mono} , of approx. 1, and the value obtained on the ordinate is not negative. The BET analysis can be applied very well to BET constants between 100 and 200. This is where a clear bend in the adsorption isotherm (types II or IV) appears at a relative

pressure of approx. 0.1. For microporous substances (BET constant above 200), such as activated carbon, the BET surface only provides information about the sum total of the outer surface and the inner surfaces of the macropores and mesopores, and, in part, of supermicropores, depending on the adsorbate used [2, 6, 7].

2.3.3 Dubinin-Radushkevich Isotherm

On the basis of the potential theory proposed by Polanyi, the Dubinin-Radushkevich equation, Eq. 9, describes adsorption as a function of the adsorption potential, $A = RT \ln(p/p_0)$.

$$\ln(V_{ads}) = \ln(V_0) - BA^2. \quad (9)$$

The prefactor, $B = (\beta E_0)^{-2}$, involves the characteristic energy, E_0 . The parameter β is dependent only on the adsorptive, and equals unity for benzene as the reference adsorptive. The characteristic energy, E_0 , is a measure of the intensity of the interaction between the adsorbent and the adsorptive.

Resolving Eq. 9 by the adsorbed volume, and substituting the prefactor, B , and the potential, A , results in Eq. 10. For practical applications, $\ln(V_{ads})$ is plotted versus $[\ln(p/p_0)]^2$. For a potential linear range the rise, B , can be used to calculate the characteristic energy, E_0 . The micropore volume, V_0 , is obtained by converting the volume, V_{ads} , into the corresponding liquid volume.

$$V_{ads} = V_0 \exp \left[-\frac{1}{(\beta E_0)^2} \left(RT \ln \frac{p}{p_0} \right)^2 \right]. \quad (10)$$

The Dubinin-Radushkevich equation is widely used for the interpolation of adsorption data of microporous substances. As long as the adsorption potential, A , is a good description of the mean potential conditions in the pores, good matching to the measured data is possible. A better interpolation can be achieved by varying the exponent of the adsorption potential, A . For this case, the Dubinin-Astakhov equation provides for a range of the exponent between 1 and 3. For highly heterogeneous pore distributions, a Dubinin-Radushkevich equation can be set up for each characteristic potential. The sum total of all individual equations can then be used to calculate the pore distribution. Instead of a sum total, also a product of local Dubinin-Radushkevich equations and a distribution function can be used to describe the measured data. However, this involves a tremendous evaluation work as a consequence of non-linear optimization [8].

2.3.4 t-plot

t-plot: The idea of the t-plot is to compare the adsorption isotherm of the test material assumed to be a porous substance with an adsorption isotherm of the non-porous material of the same origin. Forming the quotient of the specific adsorbate volume, V_{ads} ,

of the non-porous material and the volume of the first adsorbed monolayer, V_{mono} , and multiplying it by the monolayer thickness, t_i , produces the thickness of the layer, t :

$$t = \frac{V_{ads}}{V_{mono}} t_i. \quad (11)$$

The volume of the monolayer can be calculated from Eq. 2 or Eq. 8. The plot of the thickness of the layer, t , over the relative pressure results in the standard isotherm. To characterize microporosity, the specific adsorbate volume, V_{ads} , of the test material is plotted over this thickness of the layer, t . Figure 3 shows the four possible forms of the t -plot.

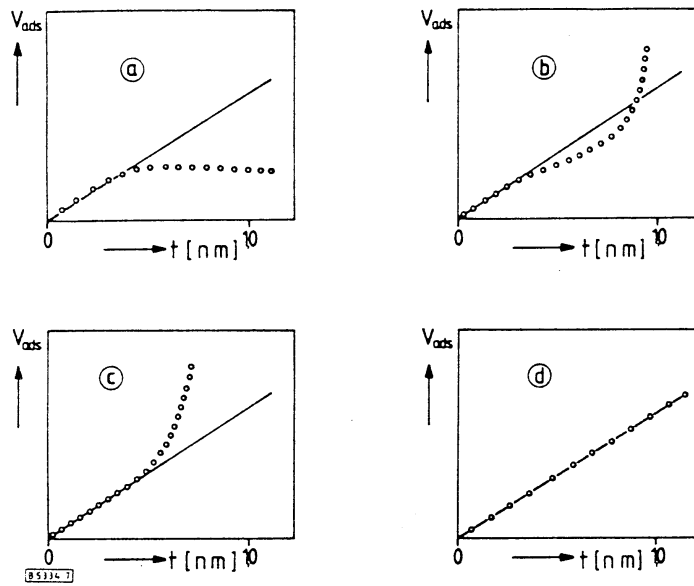


Figure 3: t -plot of (a) purely microporous, (b) microporous and mesoporous, (c) purely mesoporous, and (d) non-porous or only macroporous test materials [7].

The difficulty in producing t -plots stems from the need for a standard isotherm of the material to be studied. Various authors therefore presented matched equations not requiring a standard isotherm. De Boer is the author of Eq. 12 for calculating the thickness of layer, t , in the case of nitrogen adsorption [7, 9]. It has been used to produce t -plots in this report.

$$t = \left[\frac{13,99}{\lg(p_0/p) + 0,034} \right]^{1/2}. \quad (12)$$

2.3.5 Density Functional Theory (DFT)

One way of determining the distribution of pores in the ranges of micro- and mesoporosity (up to a relative pressure of 0.7) is offered by Density Functional Theory. The

modified non-local form often used in this case describes all pore distributions as the integral of the product of a kernel function and a distribution function. The kernel function reflects the adsorption isotherm for a porous material of a given pore width. The distribution function indicates the respective step width of the kernel function in a given quantity (e.g. pressure). The overall distribution, called Fredholm integral, results for the determination of the pore volume as a function of pressure:

$$V_{ads}(p) = \int dW q(p, W) f(W). \quad (13)$$

where V_{ads} is the adsorbed volume; W , the pore width; $q(p, W)$ is the kernel function, and $f(W)$ is the associated distribution function. To match this expression to experimental adsorption isotherms, the integral is substituted by a sum:

$$V_{ads} = \sum_i q(p, W_i) f(W_i). \quad (14)$$

The kernel function, $q(p, W)$, then is described by a matrix, $q(p, W_i)$, of the adsorbed volume for a given number of pressure levels, p , and a fixed pore width, W_i . The distribution function, $f(W_i)$, becomes a vector for the same number of pressure levels and the same pore width. The actual calculation of the pore volume per pore width is preceded by an interpolation of the measured pressure levels to the given ones. The quality of the interpolation as well as the number and distribution of the given pressure levels decisively influence the accuracy of the pore distributions obtained and, in particular, the pore volume determined [10].

2.4 Conclusion

The shape of an adsorption isotherm for a given adsorptive reflects the porous properties of the sorbent. However, due to the selective applicability of the different approaches, as mentioned above, the derived numbers need to be interpreted carefully. As a guideline for the experimental section in the following, Table 2 lists the typical results which are provided by the different evaluation approaches.

Table 2: Available information in dependence from the used evaluation approach

Method	Derivable information
Henry	use for blank measurements
Langmuir	surface area, monolayer volume
BET	surface area
Dubinín-Radushkevich	adsorption energy, micropore volume and surface
t-plot	micropore volume and surface, external surface
DFT	pore size distribution, total pore volume

3 Experimental Setup

3.1 Substances Studied

3.1.1 Activated Carbon

This study focussed on the SC 2 activated carbon made by Chemviron GmbH. SC2 is a granular activated carbon obtained from coconut shells and activated in water vapor. It is usually used for solvent recovery, e.g., of benzenes, alcohols, chlorinated hydrocarbons, esters, ketones, and other hydrocarbons, from vapors and solutions. Moreover, SC 2 is used as a catalyst or catalyst carrier in exhaust air cleaning, in cigarette filters, and in face masks [11]. For the cryosorption applications of interest in this report, SC 2 has been screened in a special qualification programme and demonstrated to have the best pumping performance of over 400 samples [12].

From the information provided by the manufacturer, this activated carbon has these characteristics:

Table 3: Physical properties of SC2 activated carbon [11].

Bulk weight (densest packing)	0.45–0.48	g/cm ³
Particle density (Hg displacement)	0.80–0.85	g/cm ³
Actual density (He displacement)	2.0–2.2	g/cm ³
Void volume at densest packing	38–42	%
Specific heat at 100°C	0.80–1.00	$\frac{\text{kJ}}{\text{Kkg}}$
Ash content	1–4	%
Hardness coefficient	95–99	%
Moisture (when packed)	0–2	%
Iodine value	1200–1300	mg/g
Carbon tetrachloride adsorption	60–70	%
Benzene value	36–40	%
Size (sieving analysis)	< 0.6 mm	5 %
	> 1.7 mm	10 %
	in between	85 %

3.2 Gases Used

In accordance with the requirements for nuclear fusion, helium and hydrogen gases were used as adsorptives. As a number of methods (such as BET) have become established standards in the characterization of porous substances, experiments with nitrogen were run as well. The helium and nitrogen gases were used in a purity of 99.9999 vol.%, hydrogen with a purity of 99.999 vol.%.

In these studies and evaluations, the following numbers were used for the critical temperature, T_c ; the critical pressure, p_c ; the saturation vapor pressure, p_0 , with the normal boiling temperature (T_0) and the molar mass, M [13]:

Table 4: Selected data of the gases used

Gas	T_c [K]	p_c [kPa]	p_0 [kPa](T_0 [K])	M [g/mol]
H ₂	33.19	1315.20	101.04 (20,38)	2.0159
He	5.20	227.46	99.40 (4,21)	4.0026
N ₂	126.19	3397.80	101.35 (77.35)	28.0134

3.3 Measurements

The measurement of sorption isotherms aims at determination of the amount adsorbed vs. pressure at a given temperature. The standard way to do this, is a volumetric process, in which a gas is added to the adsorbent either stepwise or continuously. When the gas is fed step by step (static expansion process), it is filled into an interim volume separated from the recipient containing the adsorbent. When the required pressure in the interim volume has been reached, the gas is expanded in the adsorbent recipient. The pressure and the time are recorded when equilibrium has been reached. The gas volume adsorbed can be calculated from the gas volume admitted and the dead volume determined by blank measurements.

In the dynamic volumetric technique, the adsorptive is fed to the adsorbent through a flowmeter. The gas volume admitted is determined not from the size of the interim volume and the pressure, but from the flow rate and the time. A quasi-steady state equilibrium is achieved when the volumetric flow rate is clearly below the adsorption rate. The volume of gas adsorbed again can be calculated from the volume admitted and the dead volume [14]. The latter is the method used throughout all measurements performed for this report.

3.4 Experimental Setup

The COOLSORP facility is made up of two components, a modified commercial facility for determining the surface of porous substances by the BET technique (OMNISORP 100), manufactured by the Omicron Technology Corporation (today Beckman Coulter), and a newly built part to accept the samples and generate the low temperatures required.

3.4.1 OMNISORP Unit

The OMNISORP 100 sorption measurement facility is an automatic analyzer employing the continuous volumetric method. A picture of the unit in its original state is shown in Fig. 4, a flow scheme is given in Fig. 5.

The facility can be subdivided logically. In the degassing section (H) on the left, the samples can be evacuated and heated up to 450 °C simultaneously, while the right-hand section (R, S) serves for the sorption studies. Both sections can be evacuated by means of valves 8 and 5, respectively, through a two-stage rotary vane pump (made by Edwards). A Penning vacuum tube (P) made by Edwards is installed between the rotary

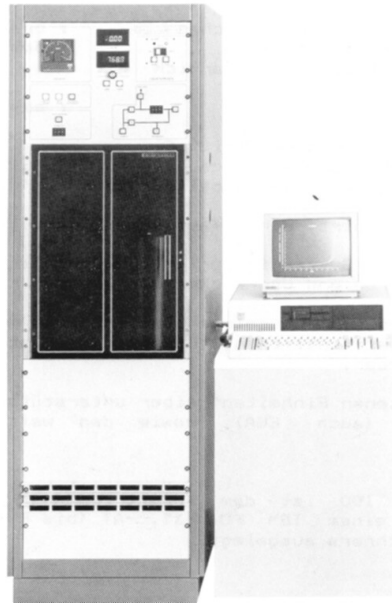


Figure 4: Front view of the OMNisorp 100 sorption measuring system.

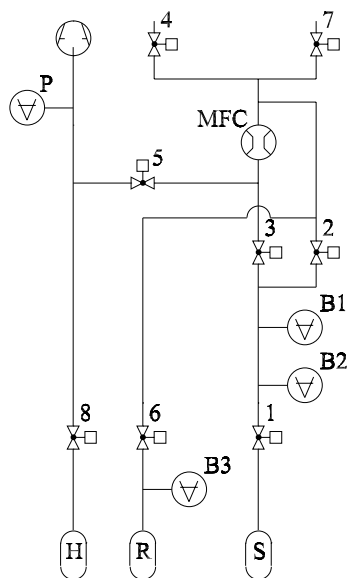


Figure 5: Basic flowsheet of the OMNisorp 100 sorption measuring facility.

vane pump and valve 5. The vacuum meter serves to monitor the rotary vane pump and the vacuum in the degassing section (with valve 8 in the open position).

The sorption part has two recipients, one for the sample material (S) and a reference recipient (R) to determine the saturation vapor pressure. Both recipients were originally surrounded by a Dewar. This was filled to a uniform nitrogen level by means of an automatic refilling control unit. The recipients can be separated from the remaining

part of the vacuum system by valves 1 and 6, respectively.

Three capacitive pressure sensors (B1–B3) of the Baratron type (made by MKS) are installed in the sorption section for pressure measurement. Two sensors working in the range between 0.1 and 1000, and 0.001 and 10 Torr are installed between the valves 1 and 3 and serve for pressure measurement in the sample space. The third sensor covering the range between 0.1 and 1000 Torr is used to determine the saturation vapor pressure. It is located between the reference recipient and valve 6. Together with the pressure sensors, the mass flow controller (MFC) is installed in a temperature-controlled housing. It is kept at a constant 40 °C by means of an electric heater, a fan, and a thermocouple. The mass flow controller made by Brooks allows nominal gas flows to be set in the range between 0.3 and 5 sccm.

The sorption section also contains valves 4 and 7 for separating the vacuum section from the gas supply, and valves 2 and 3. The latter valves determine the path of the gas flow through the mass flow controller. When the adsorption isotherm is recorded, valve 3 is open, valve 2 is closed; the situation is the other way around with desorption measurements.

The OMNISORP 100 sorption facility allows automatic measurements of adsorption and desorption isotherms. The software package coming with the analytical setup includes more programs for evaluating the measured results (BET, t-plot and the like) which, however, are designed only for the evaluation of nitrogen isotherms at 77 K [15].

The conversion of OMNISORP 100 for integration in COOLSORP comprised the removal of the Dewar (nitrogen pool), replacement of the sample vessel by a gas transfer line to the new sample recipient, replacement of the reference recipient, and linking the vacuum pump rig of the low-temperature section to the vacuum section of OMNISORP 100.

3.4.2 Refrigerator Unit

The refrigerator unit is required for cooling the samples under study to temperatures between 4 and 77 K. It replaces sample cooling by liquid nitrogen (77 K as a minimum) of the OMNISORP unit. Figure 6 and 7 show a front view and the schematic design of the refrigerator unit.

The key part of the new plant section is the SRDK-408EW-H cryocooler made by Sumitomo. It consists of a two-stage cryohead (1), a compressor (2), and two transfer lines. Depending upon the heat input, the cryohead attains temperatures down to 3 K at the second stage and approx. 30 K at the first stage. The thermal load of the second stage is reduced by means of a vacuum insulation and by a radiation shield (3) at the first stage. The temperature of the second stage can be increased by the 100 W heater attached to that stage. The controller used is a temperature controller (4) made by Lakeshore (model 340) which measures the temperature by means of a silicon diode (DT-470) mounted to the second stage.

The second stage also holds the sample recipient connected to the OMNISORP 100 unit by means of a gas transfer line (6). The pump rig (7) serves to generate the insulating



Figure 6: Front view of the refrigerator unit.

vacuum in the vacuum recipient (5) and also to generate the vacuum in the sample recipient. The cryohead and the vacuum recipient are mounted to the support rack (8) which also carries the crane arm (9). It serves to lift the vacuum recipient during sample changes and maintenance work.

3.5 Experimental

The experimental part is subdivided into three subsections: preparation, measurement, and processing of the measured data. The first step of sample preparation is heating and weighing. For this purpose, the sample is filled into a stainless steel recipient and degassed in the heating station of the OMNISORP facility for at least 24 hours at 100°C. Afterwards, the mass is determined by means of a laboratory balance (type 1264MP by Sartorius, resolution 1/100 g) from the difference in masses of the recipient with and without the sample.

After the sample has been weighed, it is filled into the sample recipient (Fig. 8 shows the sample recipient with the sample filled in.) For this purpose, the vacuum recipient is opened, the radiation shield is removed, and the sample recipient is opened. After the sample has been added, the sample recipient can be closed either with a blind flange or with a flange carrying a vacuum feedthrough and a silicon diode for determining the temperature. The radiation shield and the vacuum recipient are mounted in place again, and the sample recipient is evacuated by means of the vacuum pump rig. Immediately afterwards, evacuation of the vacuum recipient is initiated. After at least 24 hours of evacuation of the two recipients, the cryohead can start to work. Until the temperature equilibrium is reached between the sample, the sample recipient, and the second stage

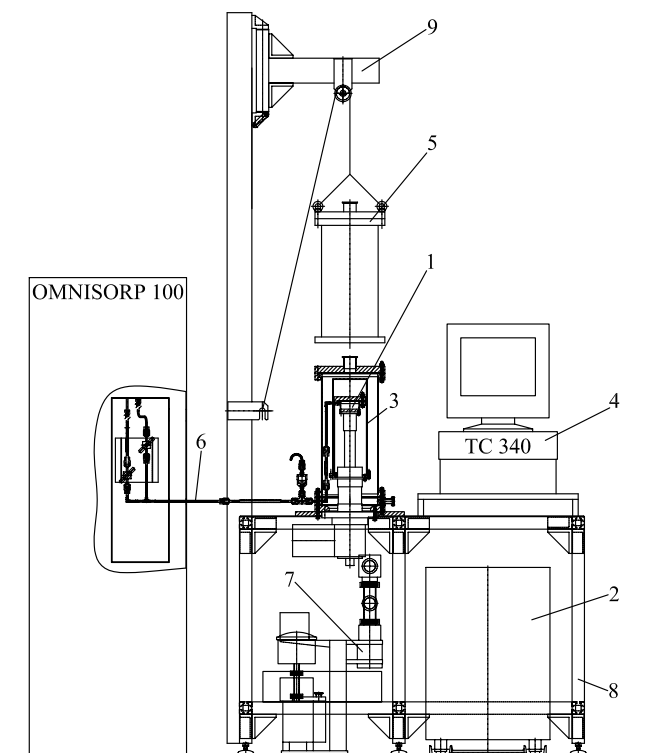


Figure 7: Schematic front view of the refrigerator unit.



Figure 8: Sample recipient with sample.

of the cryohead, temperature measurements are carried out as necessary at intervals of 1 minute by means of the diode attached to the second stage of the cryohead and, if available, the diode in the sample recipient. The resultant temperature-time curves serve for checking the temperature balance. If a higher temperature is required, and the temperature is underrun, the heater attached to the second stage of the cryohead can be activated by means of the temperature controller.

The measurement breaks down into recording the flow rate, the temperature and the pressure for adsorption and, as an option, subsequently for desorption. The first step in measurement is a check of temperature (temperature-controlled section of OMNISORP

and the sample), pressure (sample recipient and isolating vacuum), and of the communication between the measuring units and the control computer. As required, the appropriate program points are called up. Then all valves are closed. The appropriate point on the menu can be used to start the adsorption and/or desorption measurement after the measuring parameters have been entered. In this case, the valves are controlled, and the measured data recorded, automatically.

The end of the measurement is marked by reaching a given pressure level or a maximum period of time. Depending on whether the sample material is to be changed, the sample recipient must be heated to room temperature, and both recipients must be vented, or the sample recipient is evacuated again for degassing the sample. The next measurement follows after the sample material has been degassed.

3.5.1 Evaluation of the Measured Results

Several approaches were made to evaluate the measured results: The first possibility involves the software coming with the OMNISORP facility. It includes programs for determining the BET surface, plotting the adsorption isotherm, plotting a t-plot and the like. As the software is matched to the adsorption of nitrogen at 77 K, the evaluation by this way is limited on that measurement. As it is no longer possible to directly measure the saturation vapor pressure after the conversion of OMNISORP 100 to COOLSORP, the equation of state was employed for used gases [13].

The other possibility of evaluation results from the use of table calculations and mathematically orientated software. The software presented in [8] contains a variety of tools for use in determining materials data. For this purpose, the measured data files must be converted into a format readable for table calculation by means of a utility of the measurement software of OMNISORP. Moreover, the dividing signs in the tables must be converted. In this table calculation, the adsorption isotherm is calculated. In order to take into account the non-adsorbed volume, a dependency of the time, t , on the measured pressure, p , is determined out of the helium isotherm at 77 K (with the sample) and the helium isotherm of the blank measurement at the corresponding temperature by means of linear regression. The parameter, a_{He} , obtained for the rise of the regression line allows the time to be calculated which is necessary to reach the appropriate pressure.

The total volume filled in, V , can be calculated from the product of the flow rate, \dot{V}_{ads} , and the time, t . The volume, $V_{ads,i}$, adsorbed at a specific time, t_i , now can be calculated as the difference between the total gas volume filled in, $\dot{V}_{ads} \cdot t_i$, and the non-adsorbed volume, $\dot{V}_{ads}(a_{He} p_i)$:

$$V_{ads,i} = \dot{V}_{ads} \cdot (t_i - (a_{He} p_i)). \quad (15)$$

This equation must be corrected for two cases: If the flow rates during the blank measurement and during the actual measurement differ from each other, the respective quotient, $\dot{V}_{ads}/\dot{V}_{He}$, is substituted in Eq. 15 to correct for the blank measurement. The other correction results from the real-gas properties of the adsorptives used. On the basis of

Eq. 16, the compressibility factor, Z , was developed by a second-degree polynomial in p and linked to the blank volume by multiplication [16]:

$$\frac{pV}{nRT} = Z, \quad \text{mit} \quad Z = 1 + B'p + C'p^2. \quad (16)$$

$$V_{ads,i} = \dot{V}_{ads} \cdot \left(t_i - \frac{\dot{V}_{ads}}{\dot{V}_{He}} \cdot \left(1 + B'p + C'p^2 \right) \cdot (a_{He} p_i) \right). \quad (17)$$

Equation 17 furnishes the adsorbed volume under standard conditions ($p = 1013.25$ mbar, $T = 0^\circ\text{C}$), while the blank volume of a real adsorptive at the measured pressure and the test temperature was taken into account.

Another correction is applied to the pressures measured to consider the thermal transpiration effect [17, 18]. It takes into account the differential pressure according to the difference in temperatures of the pressure sensor and the sample recipient ($\Delta T = 308, 8$ K max.). However this influence is quite small. The largest for Helium at the lowest pressure and 4 K is a correction of about 10 %.

The adsorption isotherms as obtained by means of Eq. 17 constitute the basis of other calculations, such as the Langmuir plot and studies of the dependence on temperature and type of gas of the adsorption process.

An additional way of evaluating the measured results makes use of the Autosorb1 software produced by Quantachrome Corp. This software is a measurement and evaluation programme, which offers a broad spectrum, from simple plotting the adsorption isotherm to sophisticated DFT application. Again, the input data files had to be adapted to the requirements of the software.

3.6 Operational Studies

The operational studies include all work necessary to run the measuring equipment. In addition to tests of the leaktightness of the experimental setup and the functioning of all parts, the properties of the cryocooler were examined, and the necessary calibration and blank measurements were conducted.

3.6.1 Calibration

Quantitative analysis of the samples, especially with regard to calculation of the BET surface, micropore distribution and micropore volume, requires precise determination of the pressure in the sample recipient and of the mass flow rate. However, as the respective capacitive pressure gauges and the mass flowmeter were contained in a closed, temperature-controlled box, calibration was only possible in-situ. The reference standards required for this purpose were integrated into the gas transfer line (Fig. 7, item 6).

The reference standard used to calibrate the pressure sensors was a new capacitive pressure gauge of the same design calibrated by MKS. During calibration, the output voltages of the individual pressure measuring units (B1–B3, Fig. 5) in OMNISORP 100

were compared, by means of the measurement software, with those of the calibrated pressure sensor (Fig. 9). Within the range of measurement (B1 and B3: 0.1-1000 Torr; B2: 0.001-10 Torr), a linear relationship was found between the output voltage and the reference voltage for the three pressure measuring instruments. Attaining a maximum voltage for Baratron B2 therefore results from the narrower range of measurement (10 Torr as compared to 1000 Torr). Moreover, the influence of voltage division within the OMNISORP plant section is evident. The maximum output voltage of 10 V of all pressure sensors decreases to approx. 3 V in B1, and to approx. 2.6 V for B2. The measured results represented in Fig. 9 served as a basis for linear regression. The values obtained in this case for the rise and zero shift were integrated into the measurement software for correction of the readings.

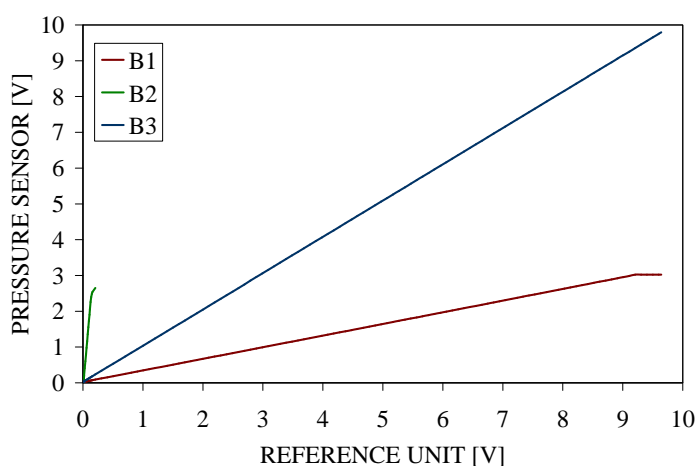


Figure 9: Voltage output of the pressure sensors compared to the calibration reference.

A Brooks Vol-U-Meter was available for calibrating the mass flowmeter. In this unit, the displacement of a piston sealed with mercury is used to measure the volume of gas flowing through the mass flow controller. After conversion of the measured volume to standard conditions ($p = 1013.25 \text{ mbar}$, $T = 0^\circ\text{C}$) the mass flow is determined from the standard volume and the measuring time. Calibration was carried out for the relevant mass flows and for nitrogen and helium as gases. Figure 10 shows the result for nitrogen. One striking feature is the pronounced deviation from the average of some readings. This effect is probably due to an incomplete opening of the solenoid valve in the flowmeter. Consequently, these data were not taken into account in calculating the flow rates. For helium, the resultant flow rates were seen to be a factor of 1.4 higher as on average. For measurements with hydrogen, the values for nitrogen were corrected by a factor of 1.01 [19].

3.6.2 Studies with the Cryohead

The cooling and heating behavior of the cryohead with and without a sample recipient and temperature control by the temperature controller made by Lakeshore were studied.

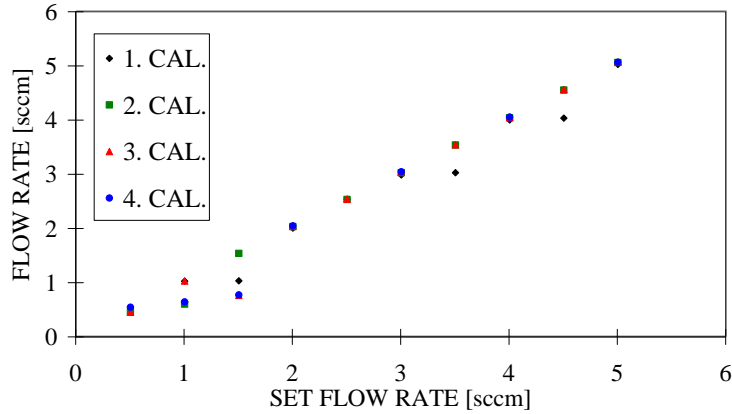


Figure 10: Comparison of the set flow rate with the flow rate determined for nitrogen, converted to standard conditions (273,15 K, 1013,25 mbar).

Cooling and Heating The first measurement to be recorded was the cooling curve without a sample recipient. For this purpose, the temperature level of the diode at the second stage of the cryohead was read from the temperature controller and stored together with the time. In the same way, several cooling curves were plotted for the cooling curve with a sample recipient, and were averaged. Figure 11 shows the results. The difference in the cooling phase due to the heat input into the sample recipient is evident. As a consequence, time for delayed cooling of the sample recipient was added to the time required by the second stage to cool, and a corresponding minimum cooling time was established prior to each measurement.

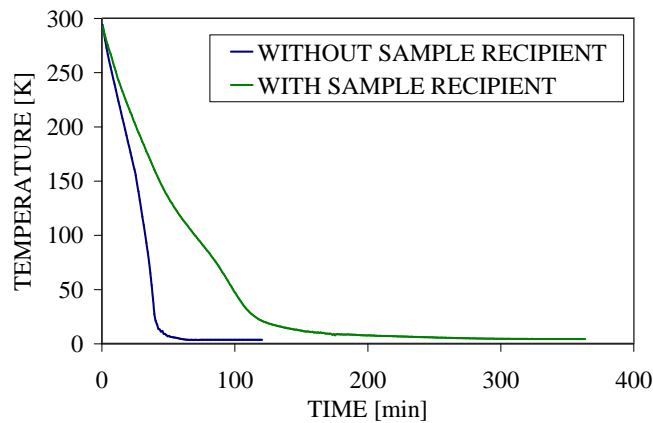


Figure 11: Cooling curve with and without a sample recipient.

A test of the insulation quality of the vacuum and the radiation shield was made by monitoring the warm up of the coldhead after switching of the refrigerator. Fig. 12 shows a very slow temperature rise, which demonstrates the good thermal insulation.

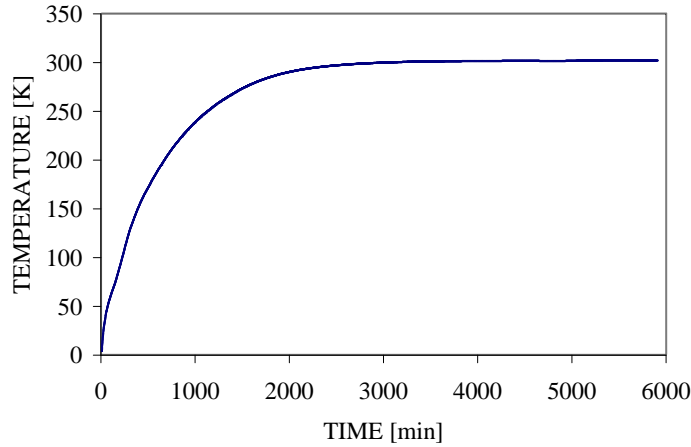


Figure 12: Warm up under thermal insulation conditions.

Temperature Control Temperature control of the second stage of the cryohead was achieved by means of a temperature controller made by Lakeshore and an electric heater installed right under the second stage. The temperature controller supplies a varying heater current at a given voltage as a function of the preselected temperature. The control behavior can be varied by means of four parameters. In addition to three parameters for PID control, also constant heating power can be preset. In the first few studies, therefore, the attainable temperature was determined as a function of the heating power (Fig. 13). For this purpose, the values of the proportional, integral, and differential members were set equal to 0.

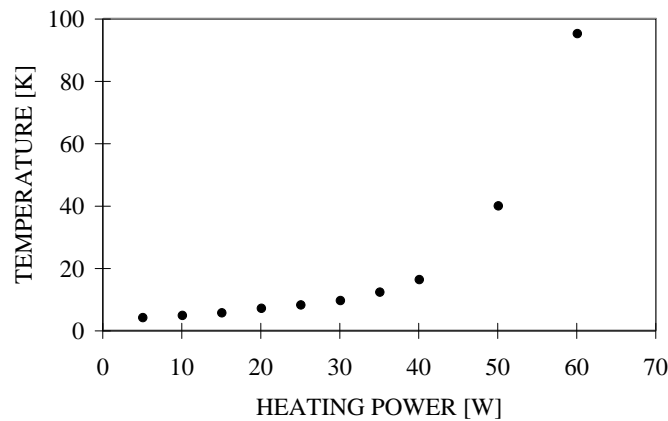


Figure 13: Attainable temperature as a function of the heating power set.

Evaluation indicated that heating powers of approx. 5–56 W are required for the range of temperatures under study of 4–77 K. Here the temperature levels of 4.21 K for the adsorption and desorption studies with helium, and 77.35 K for experiments with nitrogen are of particular interest. For these two temperatures, the values for the propor-

tional, integral, and differential members were varied within a range of 10–90 %. As a consequence of the temperature fluctuations due to the permanent decompression and compression in the piston of the second stage, the temperature control was designed to be very dynamic with a P of 80–90 %, an I of 50–60 %, and a D of 80–90 %. No constant heating power was preset.

For the temperature of 4.21 K, this allowed the temperature fluctuations to be attenuated to max. ± 0.15 K, while the mean temperature is in excellent agreement with the preset level (Fig 14). For a set level of 77.53 K, only very minor temperature fluctuations are seen (less than 0.1 K). The levels mentioned above for P, I, and D, however, result in the temperature being reached very quickly.

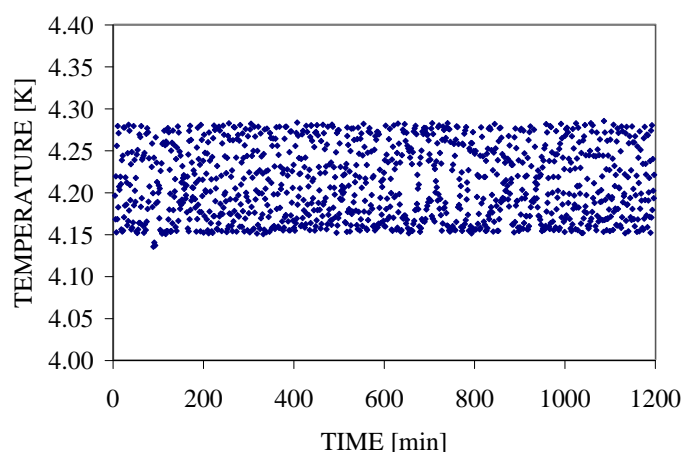


Figure 14: Temperature fluctuations at 4 K.

3.7 Blank Measurements

Blank measurements at various temperatures were carried out to determine the volume of the facility. The approach used is that employed for experiments with samples. The measured pressure and time levels constitute the basis for linear regression. The outcome is a dependence on pressure of the measuring time. As the product of time and flow rate is equal to the non-adsorbed volume, Eq. 17 can be employed to determine the adsorbed volume from the rise, a_{He} , determined from the regression. Any other corrections necessary were carried out as described in Section 3.5.1 above. For example, Fig. 15 shows six blank measurements in the range of 4–40 K. The pronounced curvature of the blank measurement at 4 K is due to the higher real gas correction near the critical point (5.20 K, 227.46 kPa) compared to the other blank measurements.

A total of 25 blank measurements were recorded, at least two of them by using helium for each experimental temperature, and one each with hydrogen at 20 K and nitrogen at 77 K. The two latter ones were performed for control purposes.

This large numbers of measurements enabled us to produce a fine map of blank corrections. It should also be emphasized that the term volume here does not assign a

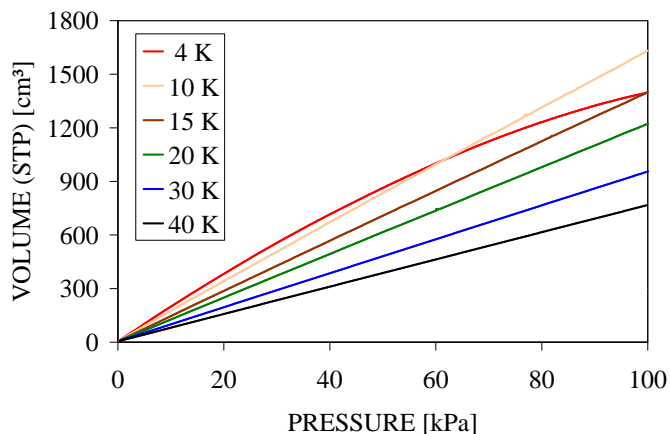


Figure 15: Blank measurements with helium in the range of 4–40 K.

mechanical volume, which would be more or less constant despite of thermal contraction effects, but it denotes an amount of gas stored in the facility at changing pressures and temperatures.

3.8 Dependence on the Flow Rate

The continuous volumetric process includes constant feeding of the adsorptive. For this reason, the question had to be clarified to what extent a different flow rate influences the measured results. Thus, measurements with varying flow rates were run at 77 K (determination of the blank volume) and 4 K. The results of the experiments at 4 K are shown in Fig. 16.

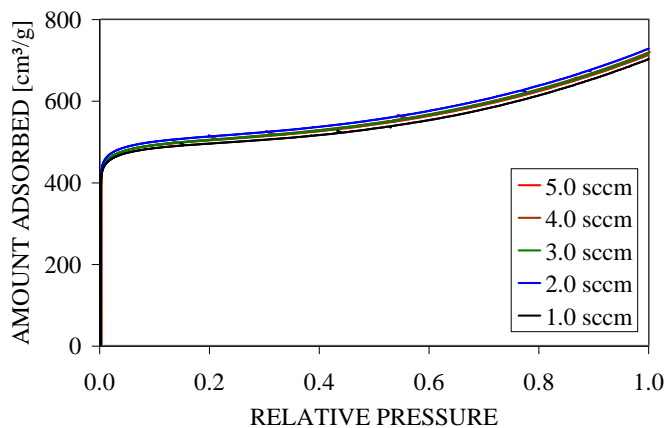


Figure 16: Adsorption isotherms for helium at 4 K for various flow rates.

The differences between the measurements both for 4 K and for 77 K are only weak. Moreover, no ranking order by flow rates was ascertained. For the following measure-

ments, a flow rate of 2 sccm of nitrogen equivalent was chosen, which corresponds to a flow rate of 2.85 sccm for helium. The value of 2 sccm represents an optimum with respect to the duration of the experiment (less than 24 h) and the stability of the mass flow controller as well as the requirement for a quasi-steady thermal equilibrium during the experiment.

3.9 Encountered Problems

During the preliminary studies and the experiment, problems arose in the experimental procedure, especially in the OMNISORP 100 section. Although the tests of the measuring software had been successful, the first problems arose in the executability of the routines. Because of problems believed to exist in the control computer, the computer was replaced completely. After reinstallation of the measuring software, the problems no longer occurred, except for a few sporadic errors.

Another error was caused by the hardware in OMNISORP 100. In that case, the analog signals corresponding to the readings were no longer updated. The measuring software did not recognize the error and did not generate the appropriate error signal. As the problem occurred only sporadically in a few measurements, it was not possible to detect the cause. In most cases, restarting OMNISORP 100 and, subsequently, the measuring software helped.

Continued problems were caused by the compressed-air valves used in OMNISORP 100. They open or close the control valves installed in the gas supply line (Fig. 5, 1–8). All valves had to be replaced because of leakages.

Also the mass flowmeter had to be replaced. The solenoid valve did not open the way it should have. As also the relationship between the valve opening and the setting of the valve was not reproducible, this defect could not be repaired even by recalibrating the mass flowmeter.

In the new section of the facility, the vacuum feedthrough and the diode attached to it for temperature measurement caused problems. The feedthrough is to seal the sample recipient vacuumtight, which was no longer the case after some preliminary tests. The diode attached at this point had been planned to check the temperature in the sample recipient and for reference compared to the temperature measurement at the second stage of the cryohead. It often supplied levels which were far too high; for this reason, the feedthrough and the diode were replaced by a blind flange.

The temperature controller made by Lakeshore showed intermittent interruptions in controlling the heating power (PID control). These interruptions resulted in a pronounced temperature increase which, in turn, led to a pressure increase in the sample recipient because of gas desorption in the sample. When the accumulating pressure was higher than the final pressure preselected in the control software of OMNISORP 100, the measurement was terminated immediately. For the rest, clear peaks appeared in the pressure-vs.-time plot of the measurement. Figure 17 exemplifies pressure rise for a measurement with helium at 20 K. The defect was repaired by replacing the flash ROMs and by reimporting the basic software of the temperature controller.

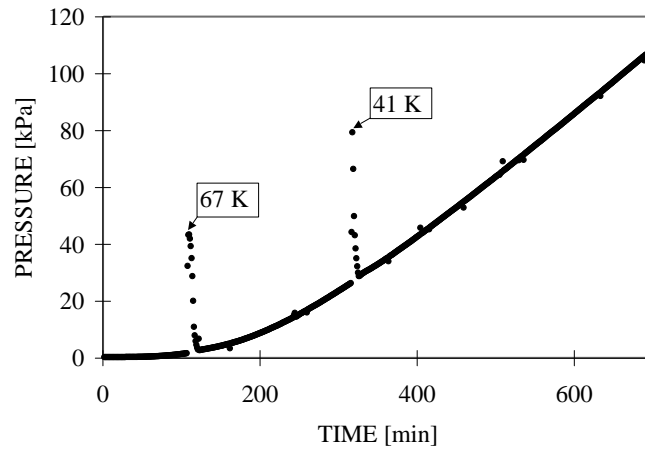


Figure 17: Pressure increase in a measurement (20 K, helium) as a result of two temperature rises.

As a result of the defects and errors listed here, some measurements had to be discontinued, and the COOLSORP facility was down for a couple of weeks. For this reason, the planned activities had to be postponed and scaled down, respectively.

4 Results

All results shown here are based on the measurements in the COOLSORP facility of two samples (samples A and B) of the SC 2 activated carbon by Chemviron. The first sample was supplied in 1990, the other in 1999. Both have identical particle sizes (12x30 US mesh, 0.6–1.7 mm) The first sample (A) was used to investigate nitrogen and helium; for the second sample (B), hydrogen was added to the test program. The chosen temperature levels include the normal boiling temperatures of helium (4.2 K), hydrogen (20.4 K), deuterium (23.7 K), neon (27.1 K) and nitrogen (77.4 K). A summary of the test program is shown in Tab. 5.

Table 5: Test program

Gas	Temperature	Sample	
nitrogen	77.4 K	A (1 run), B (1 run)	
	4.2	A (2 runs), B (5 runs)	
helium	10.0 K	A (2 runs)	
	15.0 K	A (1 run)	
	20.0 K	A (1 run)	
	20.4 K	B (1run)	
	30.0 K	A (2 runs)	
	40.0 K	A (1 run), B (2 runs)	
	77.4 K	A (2 runs), B (6 runs)	
	hydrogen	16.0 K	B (1 run)
		20.4 K	B (1 run)
		23.7 K	B (1 run)
		27.1 K	B (1 run)
		40.0 K	B (1 run)
		77.4 K	B (1 run)

4.1 Studies with Nitrogen

4.1.1 Adsorption Isotherms

A nitrogen isotherm was plotted for samples A and B and compared with the measurements of the same sample material conducted by the University of Mainz [20] and by the NBC Department of the Belgian Army [21, 22]. All samples were of SC 2 carbon, but the NBC samples had considerably lower masses of only 0.63 to 0.84 g compared to our samples, which had masses of 2.73 (A) and 2.42 g (B). The results are shown in Fig. 18.

The seven samples exhibit a type-I isotherm with an almost vertical rise at low relative pressures, and a pronounced plateau at relative pressures approx. above 0.1. For the seven isotherms there is a difference in the height of the plateau which has not been explained. On the one hand, differences in the samples may be a reason despite identical

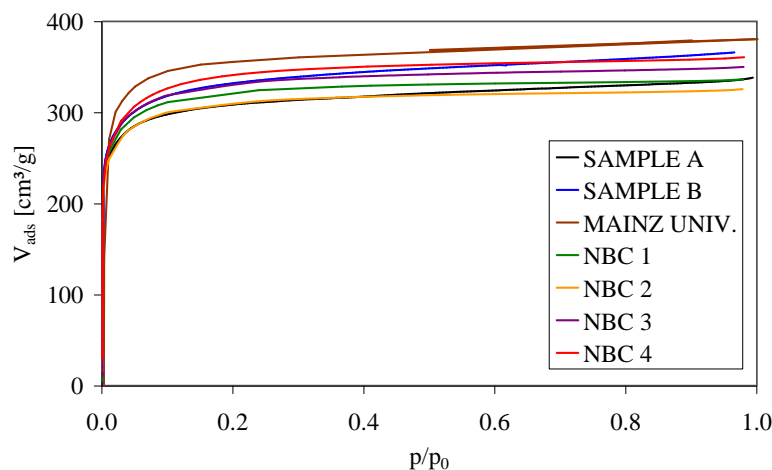


Figure 18: Adsorption isotherms for nitrogen at 77 K.

production processes. On the other hand, there are deviations due to the measuring equipment and methods of measurement. However, it is striking to see that the sample with the smallest quantity of material (University of Mainz, 0.1862 g) had the largest adsorbed volume per unit mass. This is contradicted by the distribution of the NBC samples, as no order by mass (0.63–0.84 g) or by the volume dosed (5–20 cm³/g, static volumetric process) can be seen. However, as both the samples A and B and the NBC samples are in the same range, while the methods of measurement and the measuring equipment are different, it is concluded that materials properties differ due to production processes.

4.1.2 Langmuir Plot

Figure 19 shows the Langmuir plot for six samples (cf. eq. 2). (The sample measurements conducted by the University of Mainz were not taken into account because of the absence of measured data.) The plot shows an approximately linear course except for the range of relative pressure below 0.001. For the linear regions, regressions were performed, and the monolayer volume and the resulting surfaces of the different samples were calculated (Table 6).

Both the monolayer volume and the calculated total surfaces vary by up to 10%. The deviations probably are due again to different materials properties of the samples. Because of the good regression coefficients, numerical errors in the fitting procedure are more likely to be small.

4.1.3 BET Plot

As a standard procedure of characterizing porous materials, the measured results were evaluated also by this method. Figure 20 shows the best fit of the measured results by the BET equation, which, however, still shows deviations from linearity. For this

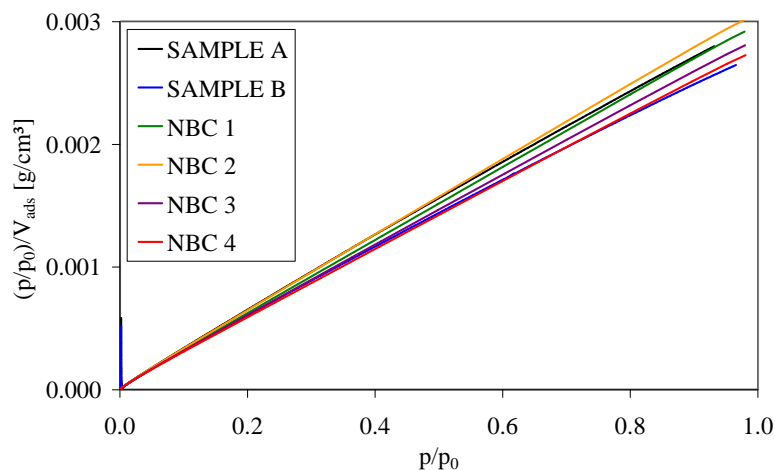


Figure 19: Langmuir plot for nitrogen at 77 K.

Table 6: Monolayer volume and total surface for the samples studied with nitrogen as determined with the Langmuir method.

	Monolayer volume cm ³ /g	Surface m ² /g
Sample A	407	1418
Sample B	387	1349
NBC 1	417	1452
NBC 2	403	1403
NBC 3	434	1511
NBC 4	448	1559

reason, evaluation was limited to an approximately linear region in the lower pressure range. The results can be seen in Table 7.

Comparing the values from Table 7 with the manufacturer's data of 1150–1250 m²/g [11] shows agreement only with the results obtained by the University of Mainz. The BET surfaces of the NBC Dept. measurements are at the upper end, while lower values were calculated for samples A and B. The differences are seen to be due to insufficient matching of the measured results by the BET process. It must be emphasized again that the BET approach is, physically speaking, not correct to use for microporous materials. However, it has become customary to use the BET evaluation nevertheless to get a fingerprint information of the material behavior.

4.1.4 Dubinin-Radushkevich Plot

Figure 21 shows the Dubinin-Radushkevich plot. Its characteristic is an approximately linear course in the upper pressure range. For the adsorption isotherms measured by the dynamic volumetric method (samples A and B) a vertical section follows after a brief

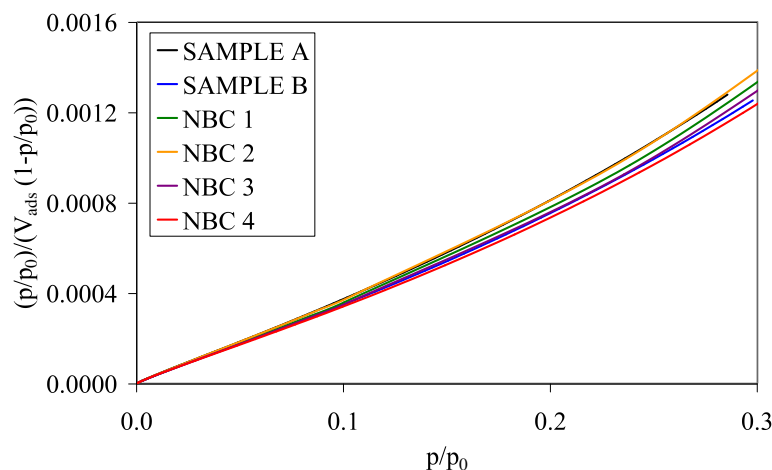


Figure 20: BET plot for nitrogen at 77 K.

Table 7: Total surface of the samples studied with nitrogen as determined by the BET method

	Surface m ² /g
Sample A	1114
Sample B	981
NBC 1	1218
NBC 2	1169
NBC 3	1260
NBC 4	1270
Mainz Univ. [20]	1172

transition. It can be explained on the basis of the continuous feeding of the adsorptive. From the first reading on, the pressure level depends on the flow rate.

A different picture is seen for the Dubinin-Radushkevich isotherms of the samples measured under steady-state conditions (NBC 1–4). In this case, the approximately linear region is extended down into the lower pressure range. In the NBC 1 samples, a clear deviation from the linear trend can be seen in the low pressure range, while this is evident already at higher pressures in the NBC 3 sample. There is no explanation of this finding. However, a dependence on the amount fed cannot be excluded.

The linear sections in the upper pressure range of the Dubinin-Radushkevich isotherms were used for calculating the adsorption energy, micropore volume and micropore surface (Table 8). The adsorption energy is in a range of 8–13 kJ/mol. For the micropore volume, the resultant value is around 0,5 cm³/g for a surface of all micropores in the range of 1200–1550 m²/g.

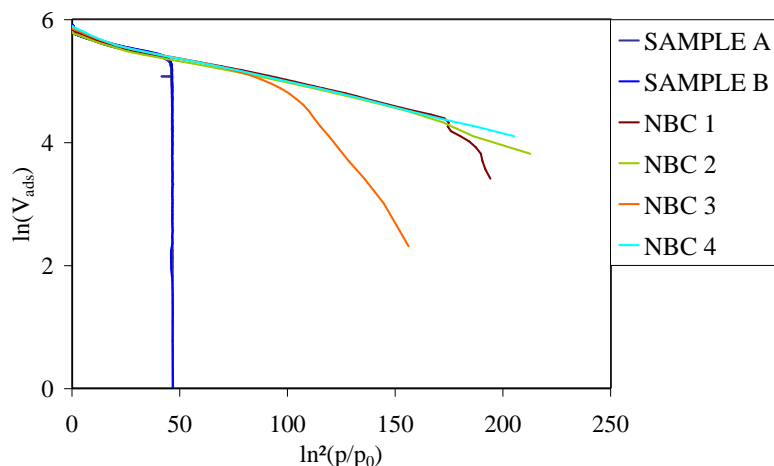


Figure 21: Dubinin-Radushkevich plot for nitrogen at 77 K.

Table 8: Results determined by the DR method for samples studied with nitrogen

	Adsorption energy kJ/mol	Micropore volume cm ³ /g	Micropore surface m ² /g
Sample A	9.37	0.4923	1386
Sample B	8.47	0.4721	1329
NBC 1	12.58	0.4612	1298
NBC 2	12.73	0.4376	1231
NBC 3	9.127	0.5281	1486
NBC 4	8.235	0.5488	1544

4.1.5 t-plot

For better characterization, a t-plot of the samples A and B as well as NBC 1–4 was derived. The curve shapes in Fig. 22 show similarities to the adsorption isotherms (Fig. 18). The approximately linear section at greater layer thicknesses was used to calculate the micropore volume and surface and the outer surface. The results are summarized in Table 9.

4.1.6 Density Functional Theory

The Density Functional Theory (DFT) is an approach to also derive the differential pore distribution information from the measured isotherm. The results are plotted in Fig. 23. An overall distribution of pores is found in the range of 6–30 Å, with pores above 16 Å contributing only very little to the pore volume. The peak values are at 10.7 and 12.5 Å. For the samples A, B, and NBC 1 a first peak is only indicated tentatively, which (excluding the NBC 3 sample) is indicative of the pores being filled already at low pressures (below $p/p_0 = 10^{-3}$). In general, the integrated pore volumes (see Table 10)

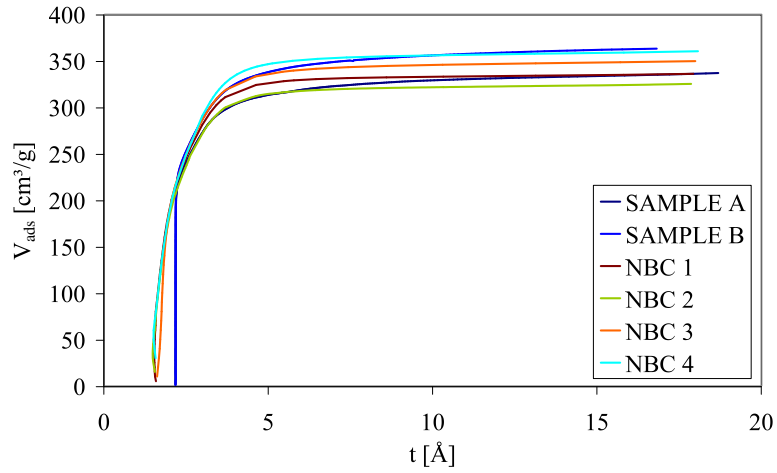


Figure 22: t-plot for nitrogen at 77 K.

Table 9: Results for the samples studied with nitrogen as determined from the t-plot

	Micropore volume cm ³ /g	Micropore surface m ² /g	External surface m ² /g
Sample A	0.4955	1100	13.7
Sample B	0.5332	963	17.6
NBC 1	0.5079	1211	6.4
NBC 2	0.4903	1162	6.7
NBC 3	0.5259	1251	8.2
NBC 4	0.5405	1259	9.2

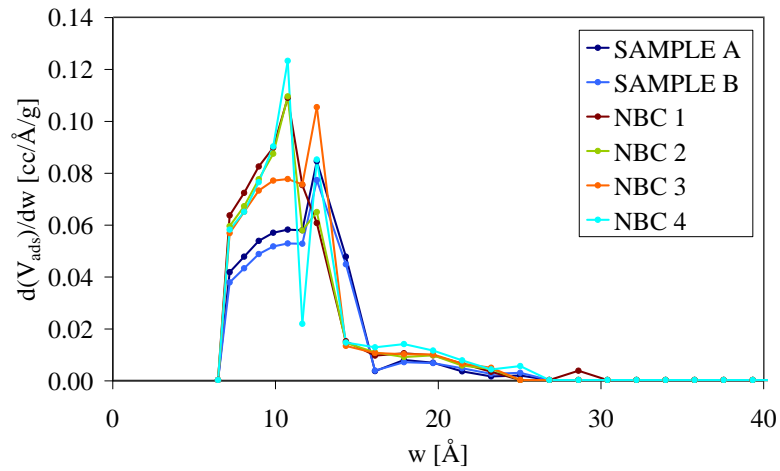


Figure 23: Differential pore distribution for nitrogen at 77 K.

of the NBC samples, which have been measured by the static expansion method, are smaller. One possible reason may be the much higher mass of the samples A and B. However, the pronounced variation cannot be fully explained in this way.

Table 10: Calculated bulk pore volumes according to DFT

	Total pore volume cm ³ /g
Sample A	0.9065
Sample B	0.9319
NBC 1	0.6875
NBC 2	0.7718
NBC 3	0.9366
NBC 4	0.8125

4.1.7 Summary of the Studies with Nitrogen

In summary, SC 2 was shown to be an almost exclusively microporous activated carbon with very narrow pore distribution. Some differences arise in the calculation of the micropore volumes. The Dubinin-Radushkevich plot and the t-plot result in micropore volumes of approx. 0.5 cm³/g, which differ greatly from sample to sample. The bulk pore volumes as determined by the DFT analysis are in the range of 0.68–0.94 cm³/g. As the pore distribution in the DFT analysis shows almost exclusively micropores (Fig. 23), the bulk pore volume and the micropore volume should roughly agree. The reason for this difference has not yet been explained.

Moreover, the micropore surfaces and the total surfaces were determined. Again, major differences are seen between the samples, on the one hand, and the methods applied, on the other hand. The calculations according to Langmuir result in total surfaces of 1350–1560 m²/g. The range of 1230–1550 m²/g for the micropore surface according to the DR method, plus the external surfaces in the range of 6.4 to 17.6 m²/g from the calculations of the t-plot, is in good agreement with the total surfaces determined according to Langmuir.

One method of good applicability has been found to be interpolation of the measured results by means of the Langmuir isotherm. Still satisfactory results were obtained by means of the Dubinin-Radushkevich isotherm and the t-plot. The BET method, even in the greatly restricted range of relative pressures of 0.05–0.1, merely showed satisfactory matchability properties to the measured results. Only because of standardization (DIN 66131) it was included in the evaluation.

4.2 Studies with Helium

4.2.1 Adsorption Isotherms

In the first test series, the dependence on temperature of helium sorption on the SC 2 activated carbon was studied. The isotherms obtained for sample A at 4.21, 10, 15, 20, 30, and 40 K are shown in Fig. 24.

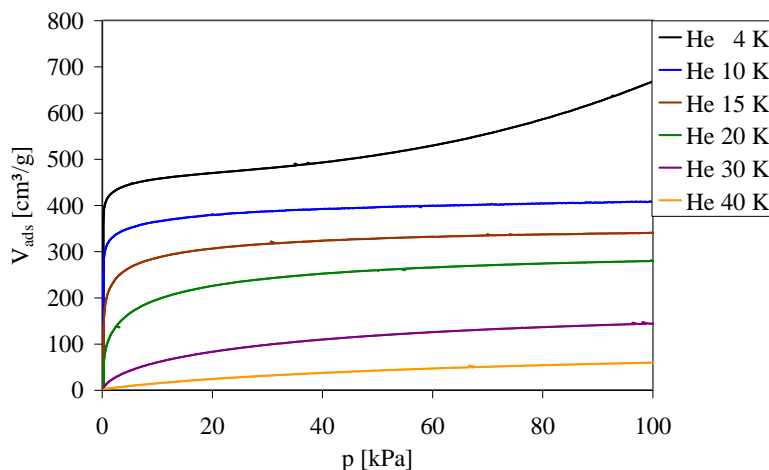


Figure 24: Adsorption isotherms for helium at various temperatures (sample A)

A striking feature, on the one hand, are the curves of the isotherms which are similar to type I (IUPAC), and the clear dependence on temperature. For the lower temperatures, there is an approximately linear decrease of the adsorbed volume with rising temperature. For higher temperatures, there is a gradually slower decrease of the adsorbed volume. At 40 K, it is only of the same order of magnitude as the non-adsorbed volume, which is why no measurements at even higher temperatures were performed. A slightly different picture is seen in the measurement at 4 K. This only isotherm in the subcritical range is more similar to IUPAC type II, which for nitrogen would indicate a mesopore material. However, this is not necessarily the case for helium, due to its lower molecular cross section.

4.2.2 Langmuir Plot

As for nitrogen, Langmuir isotherms were plotted also for the seven series of measurements with helium at 4.21 K, 2 of sample A und 5 of sample B (see Fig. 25).

The graphs shown in Fig. 25, in contrast to the studies with nitrogen, show a concave curve shape. When this difference is traced back to the average particle diameter (nitrogen 0.3 nm; helium 0.2 nm), this indicates the presence of micropores close to the mesoporous region. Because of the major deviation from linearity, no further calculations were performed.

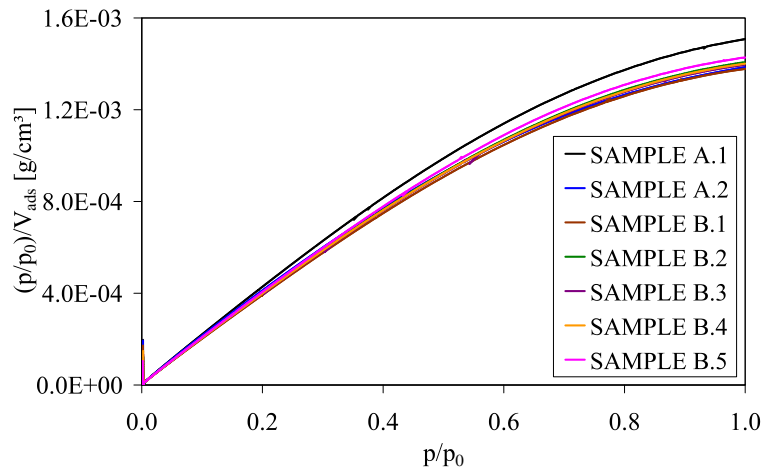


Figure 25: Langmuir plots for helium at 4.2 K (samples A and B).

4.2.3 BET Plot

The pronounced deviation from linearity of the Langmuir plot led to an evaluation of the results measured with helium in accordance with the BET method. Again, the typical range of relative pressure of 0.05–0.30 was selected. Figure 26 shows a similar characteristic as the BET isotherms did for nitrogen. As the BET method with helium does not constitute a standard, no further calculations were performed.

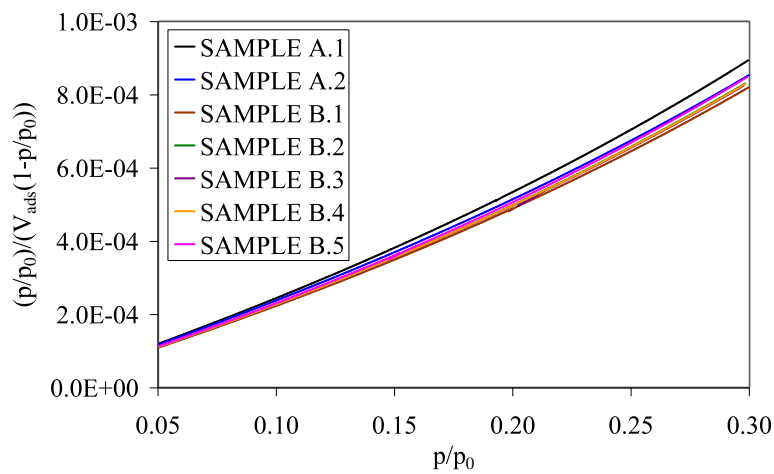


Figure 26: BET isotherms for helium at 4.2 K (samples A and B).

4.2.4 Dubinin-Radushkevich Plot

The excellent description by the Dubinin-Radushkevich equation of the results measured with nitrogen in the lower range of relative pressure led to the same studies per-

formed with helium. Figure 27 shows the corresponding plot, which illustrates results similar to that of the measurements performed with nitrogen. Regression of the linear section at lower relative pressures was the basis on which the micropore volume and micropore surface were calculated, which are summed up in Table 11 for all seven runs.

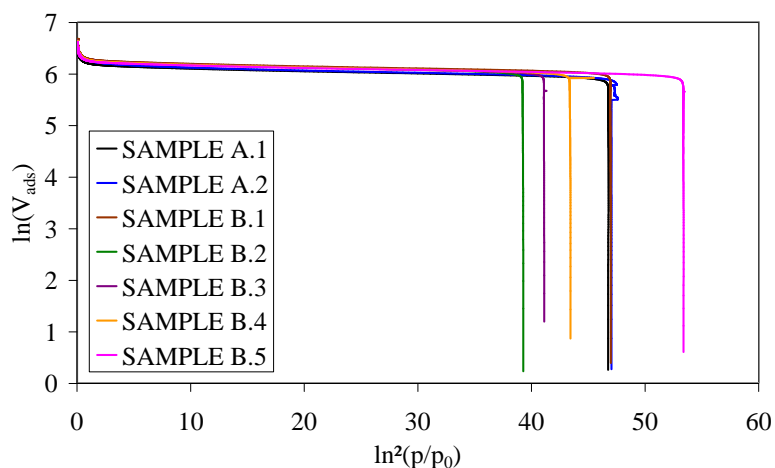


Figure 27: Dubinin-Radushkevich isotherms for helium at 4.2 K (samples A and B).

Table 11: : Results obtained by the DR method for samples studied with helium

	Micropore volume cm ³ /g	Micropore surface m ² /g
sample A.1	0.6557	1445
sample A.2	0.6720	1481
sample B.1	0.7201	1587
sample B.2	0.7097	1564
sample B.3	0.7102	1565
sample B.4	0.7086	1562
sample B.5	0.6978	1538

The values for the micropore volume and micropore surface resulting from the studies are higher than the results for nitrogen indicated in Table 8. This is because of the smaller cross section of helium, probably due to a larger attainable microvolume or closer packing in that volume. The adsorption energies were not yet estimated.

4.2.5 Summary of the Studies with Helium

The type I classification as seen for nitrogen was confirmed for helium except for the experiments at 4 K, which have a behavior closer to type II. The adsorbed volume at its normal boiling temperature of 4 K is up to a factor of 2 higher than the one of nitrogen

at its normal boiling temperature of 77 K. Still, the good applicability of the Dubinin-Radushkevich method is an indication of the microporosity of activated carbon. The higher values for the micropore volume and micropore surface compared to the nitrogen measurements are assumed to be due to the smaller mean diameter of the adsorbed gas. The presentation of the measured results according to Langmuir and BET has been found to be impractical. Evaluation by the t-plot method according to de Boer is not easily possible for helium isotherms. As in the case of the DFT method, where no corresponding kernel file is available, no calculation was performed.

4.3 Studies with Hydrogen

In view of the use of the activated carbon for pumping fusion-related gas mixes, information must be found about the competitive sorption of helium and hydrogen. The sorption of pure hydrogen was studied as a first step along this line. As in the case of helium, measurements were performed at various temperatures as listed on Tab. 5. The adsorption isotherms obtained are shown in Fig. 28.

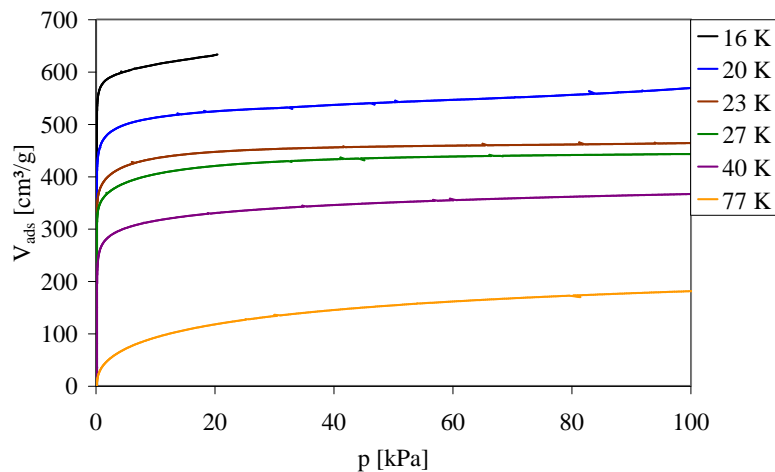


Figure 28: Adsorption isotherms for hydrogen at various temperatures (sample B).

The dependence on temperature is very similar to that of the helium isotherms. (The high pressure end of the adsorption isotherm at 16 K occurs when saturation vapor pressure is reached.) Again, the different isotherms are assigned to type I according to IUPAC. A different plot of the dependence on temperature, which is applicable for the subcritical region is shown in Fig. 29. In this case, the adsorbed volume is plotted versus the relative pressure. The shortening of the graphs in the 23 K and 27 K measurements is due to the limitation of the maximum pressure to 800 Torr (approx. 107 kPa) during an experiment.

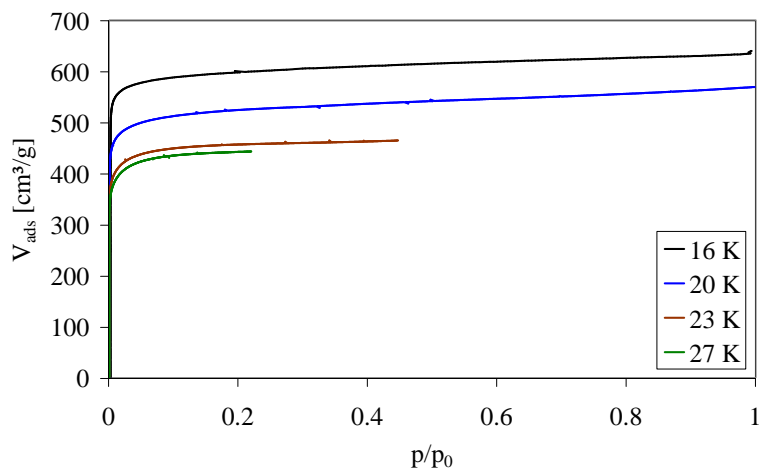


Figure 29: Adsorption isotherms for hydrogen at various temperatures in the subcritical range (sample B).

4.3.1 Langmuir Plot

The classification of the adsorption isotherms as IUPAC type I, and the comparability with the experiments with other adsorptives, were the reason to apply the Langmuir plot (Fig. 30). For this purpose, the data of the four subcritical isotherms from Fig. 29 were used. The graph shows a linear region in almost all curves which covers nearly the entire measured range of relative pressure. It was used to calculate the monolayer volume and the total surface (see Table 12).

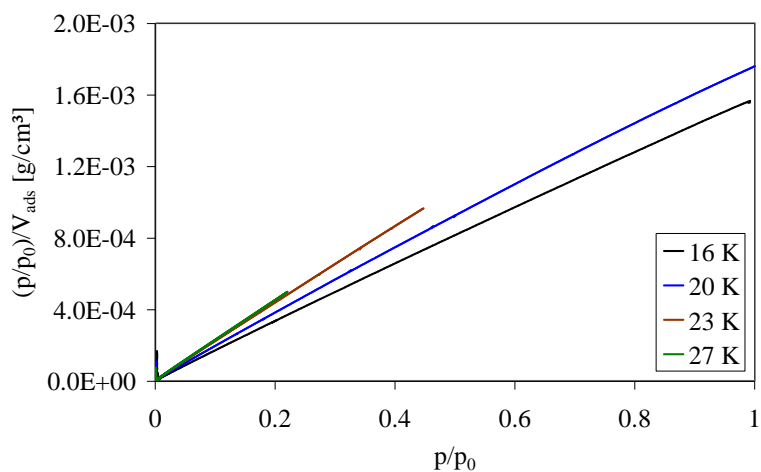


Figure 30: Adsorption isotherms for hydrogen in the plot according to Langmuir (sample B).

The results summarized in Table 12 exhibit a clear dependence on temperature. Both the monolayer volume and the total surfaces determined decrease with rising temperature.

Table 12: : Monolayer volume and total surface according to Langmuir for samples studied with hydrogen

	Monolayer volume cm ³ /g	Surface m ² /g
Sample B 16 K	629	2212
Sample B 20 K	560	1971
Sample B 23 K	464	1633
Sample B 27 K	444	1564

This pronounced dependence on temperature has not been explained so far. Moreover, surfaces calculated are significantly larger than what was calculated for helium, which is not straightforward.

4.3.2 Dubinin-Radushkevich Plot

For comparison reason, a corresponding DR plot of the four subcritical isotherms (Fig. 31) was drawn and the micropore volumes and micropore surfaces (Table 13) were calculated.

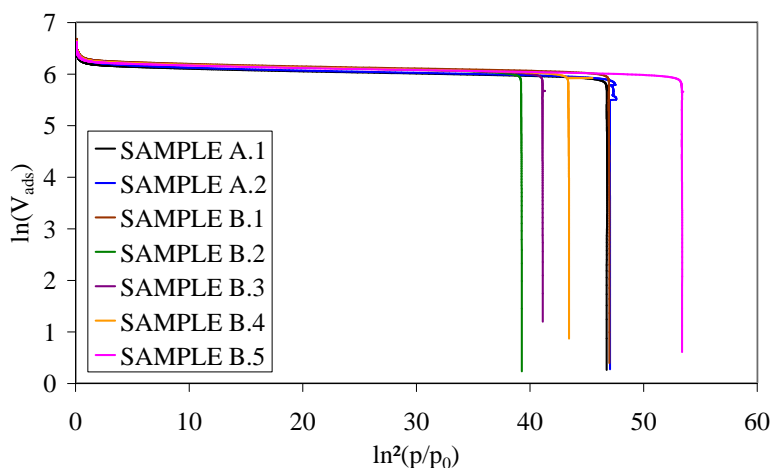


Figure 31: Dubinin-Radushkevich plot for hydrogen (samples B).

The resultant picture is essentially similar to those for the nitrogen and helium gases. The maximum contributions for $\ln(V_{ads})$ result only from the temperature-dependent peak values of the adsorbed volume, while the different maximum values for $\ln^2(p/p_0)$ are due to the different saturation vapor pressures.

A clear dependence on temperature of the micropore volumes and micropore surfaces is evident from Table 13. The value of the micropore volume calculated for the 16 K measurement lies in the range of the values determined by DFT for nitrogen. Other micropore volumes determined are similar, such as the volumes determined for helium by

Table 13: : Results determined by the DR method for samples studied with hydrogen

	Micropore volume cm ³ /g	Micropore surface m ² /g
Sample B 16 K	0.7228	2125
Sample B 20 K	0.6694	1852
Sample B 23 K	0.6280	1633
Sample B 27 K	0.6680	1589

the DR method. The continuous decrease of the micropore surface with rising temperature, however, is indicative of densities in the micropores which, unlike those used in the calculation, do not agree with the density of the liquid at the corresponding temperature. Still, there is a pronounced basic dependence on temperature which has not been explained. In general, the surfaces calculated appear to be too large. The adsorption energies were not yet estimated.

4.3.3 Summary of the Studies with Hydrogen

Like those for the other gases, the adsorption isotherms of the hydrogen experiments can be classified as IUPAC type I. The good applicability of the Langmuir and Dubinin-Radushkevich equations is another indication of the microporosity of the activated carbon. The pronounced dependence on temperature of the values determined by the two methods is still unexplained. This is where studies of the chemical surface structure should provide clarity. The calculated values of the volumes and the surfaces appear to be too high.

5 Summary and Outlook

Within the framework of Deliverable 8 of EU Task VP1 (ITER Task 448: Cryopump Development and Testing), a facility for automatic determination of the adsorption and desorption isotherms of porous substances in a temperature range of 4–77 K was built and tested. Existing instruments for pressure and flow measurements were adjusted and calibrated, respectively. Temperature measurement and control of the heating power for temperature rises were studied, and the required test parameters were determined. Moreover, the necessary repairs and conversions were made, and the vacuum section was subjected to leak testing.

After the experimental facility had been completed, the adsorption of nitrogen, helium, and hydrogen was studied in two activated carbon samples at different temperatures. The activated carbon used was the type recommended for the torus cryopump on ITER. The adsorption isotherms obtained show a clear dependence on temperature and are similar to IUPAC type I. This is an indication of an essentially microporous material. Evaluations by various methods were made to determine the total surfaces and pore surfaces and volumes, respectively. The results vary as a function of the gas and the method selected. Interpolation of the measured results by the Langmuir method (except for helium) and the Dubinin-Radushkevich equation was found to be easily applicable. Further studies must be conducted to see whether extensions of both methods (e.g. according to Tóth or Dubinin-Astakhov) can result in improvements. However, the data set presented in this study is considered to be sufficient for qualification of any new carbon material, which may be proposed in the future to replace the SC 2 material. Application of the BET equation produced unsatisfactory results, as was to be expected for an almost exclusively microporous activated carbon. However, as the BET method according to DIN 66131 constitutes a standard, variations of the BET equation will be examined in the future for better interpolation of the measured results. Moreover, variations of the t-plot and of the DFT analysis are to be studied. In the t-plot, the representation will be studied for gases other than nitrogen, while the DFT analysis is about obtaining new kernel files. At the present time, kernel files are only available for nitrogen and carbon dioxide.

Other measurements are planned as well. Deuterium is to be studied in detail as a new sorptive. Moreover, experiments with nitrogen, helium, and hydrogen are to expand the database, and measurements performed on a different activated carbon with a larger total surface are to improve comparability with measurements by other authors. The purpose of the following study would be a more exact determination of micropore distribution and of more general data, such as the total surface and the micropore surface so that, finally, a uniform picture of the SC 2 activated carbon can be obtained.

References

- [1] W. Kast, Adsorption aus der Gasphase, VCH Verlagsgesellschaft mbH, Weinheim, 1988
- [2] H. Kienle, E. Bäder, Aktivkohle und ihre Anwendung, Ferdinand Enke Verlag, Stuttgart, 1980
- [3] A. F. Hollemann, N. Wiberg, Lehrbuch der Anorganischen Chemie, Walter de Gruyter, Berlin New York, 1985
- [4] DIN 66134, Bestimmung der Porengrößenverteilung und der spezifischen Oberfläche mesoporöser Feststoffe durch Stickstoffadsorption, 1998.
- [5] F. Rouquerol, J. Rouquerol, K. S. W. Sing, Adsorption by Powders and Porous Solids, Academic Press, London, 1999.
- [6] DIN 66131, Bestimmung der spezifischen Oberfläche von Feststoffen durch Gasadsorption nach Brunauer, Emmett und Teller (BET), 1993.
- [7] S. J. Gregg, K. S. W. Sing, Adsorption, Surface Area and Porosity, 2nd edition, Academic Press, London, 1982.
- [8] D. D. Do, Adsorption Analysis: Equilibria and Kinetics, Imperial College Press, 1998
- [9] Autosorb-1 Gas Adsorption System Manual, Quantachrome Corporation, Boynton Beach, Florida, AS-1 P/N 05061, 1998
- [10] J. P. Olivier, Improving the models used for calculating the size distribution of micropore volume of activated carbons from adsorption data, Carbon 36 (1998), 10, 1469–1472
- [11] Information material SC2, SC12 und Filtrasorb 100 und 200, Chemviron Carbon GmbH, Neu-Isenburg, Germany, 1996
- [12] D. Perinic, H. Haas, A. Mack, Development of Cryosorption Panels for Cryopumps, Adv. in Cryo. Eng. 39 (1994), 1553–1559
- [13] R. T. Jacobson, S. G. Penoncello, E. W. Lemmon, Thermodynamic properties of cryogenic fluids, Plenum Press New York, 1997
- [14] J. Seifert, G. Emig, Mikrostrukturuntersuchungen an porösen Feststoffen durch Physisorption, Chemische Ingenieurtechnik 59 (1987), 6, 475–485
- [15] Instruction Manual for the Coulter OMNISORP 360/100 Analyzers, Beckman Coulter Corporation, Hialeah, Florida, 1992

- [16] Allprops Property Package, Center for Applied Thermodynamic Studies, University of Idaho, 1996
- [17] T. Takaishi, Y. Sensui, Thermal Transpiration Effect of Hydrogen, Rare Gases and Methane, *Trans. Faraday Soc.* 59 (1963), 2503–2514
- [18] W. Jitschin, P. Röhl, Quantitative study of the thermal transpiration effect in vacuum gauges, *J. Vac. Sci. Technol. A* 5 (1987), 3, 372–375
- [19] Instruction Manual for the Brooks mass flow controller model 5850E, Issue 5 (1988), Brooks Instruments Division, Hatfield, Pennsylvania
- [20] H. Reichert, *Messbericht über ausgeführte Sorptionsmessungen*, Johannes Gutenberg-Universität Mainz, 1993
- [21] Measurement data, NBC Division, Belgian Army, 2001, personal communication by P. Lodewyckx
- [22] S. Blacher, B. Sahouli, B. Heinrichs, P. Lodewyckx, R. Pirard, J.P. Pirard, Micropore size distributions of activated carbon, *Langmuir* 16 (2000) 16, 6754-6756